The VISCACHA survey – V. Rejuvenating three faint SMC clusters

E. Bica,[1]⋆ F. F. S. Maia [ID],[2] R. A. P. Oliveira [ID],[3] B. Dias [ID],[4]⋆ J. F. C. Santos, Jr [ID],[5] J. P. Rocha,[6]
L. Kerber,[6] J. F. Gardin,[5] T. Armond,[7] M. C. Parisi,[8,9] S. O. Souza [ID][10,3] and B. Barbuy[3]

[1]*Departamento de Astronomia, IF - UFRGS, Av. Bento Gonçalves 9500, 91501-970, Brazil*
[2]*Instituto de Física - Universidade Federal do Rio de Janeiro, Av. Athos da Silveira Ramos, 149, Rio de Janeiro 21941-909, Brazil*
[3]*Universidade de São Paulo, IAG, Rua do Matão 1226, Cidade Universitária, São Paulo 05508-900, Brazil*
[4]*Instituto de Alta Investigación, Sede Esmeralda, Universidad de Tarapacá, Av. Luis Emilio Recabarren 2477, Iquique, Chile*
[5]*Departamento de Física, ICEx - UFMG, Av. Antônio Carlos 6627, Belo Horizonte 31270-901, Brazil*
[6]*Departamento de Ciências Exatas e Tecnológicas, UESC, Rodovia Jorge Amado km 16, 45662-900, Brazil*
[7]*Universidade Federal de São João del-Rei, Departamento de Estatística, Física e Matemática, Campus Alto Paraopeba, Rod.: MG 443, Km 7, Ouro Branco - MG 36420-000, Brazil*
[8]*Observatorio Astronómico, Universidad Nacional de Córdoba, Laprida 854, X5000BGR Córdoba, Argentina*
[9]*Instituto de Astronomía Teórica y Experimental (CONICET-UNC), Laprida 854, X5000BGR Córdoba, Argentina*
[10]*Leibniz-Institut für Astrophysik Potsdam (AIP), An der Sternwarte 16, Potsdam 14482, Germany*

ABSTRACT

We present the analysis of three faint clusters of the Small Magellanic Cloud RZ 82, HW 42, and RZ 158. We employed the SOAR telescope instrument SAM with adaptive optics, allowing us to reach to $V \sim 23$–24 mag, unprecedentedly, a depth sufficient to measure ages of up to about 10–12 Gyr. All three clusters are resolved to their centres, and the resulting colour–magnitude diagrams (CMDs) allow us to derive ages of 3.9, 2.6, and 4.8 Gyr, respectively. These results are significantly younger than previous determinations (7.1, 5.0, and 8.3 Gyr, respectively), based on integrated photometry or shallower CMDs. We rule out older ages for these clusters based on deep photometry and statistical isochrone fitting. We also estimate metallicities for the three clusters of [Fe/H] = −0.68, −0.57, and −0.90, respectively. These updated ages and metallicities are in good agreement with the age-metallicity relation for the bulk of SMC clusters. Total cluster masses ranging from ~ 7–$11 \cdot 10^3 \, M_\odot$ were estimated from integrated flux, consistent with masses estimated for other SMC clusters of similar ages. These results reduce the number of SMC clusters known to be older than about 5 Gyr and highlight the need of deep and spatially resolved photometry to determine accurate ages for older low-luminosity SMC star clusters.

Key words: Magellanic Clouds – galaxies: star clusters: general.

1 INTRODUCTION

The Small Magellanic Cloud (SMC) cluster population is a tracer of the star and cluster formation history and chemical enrichment in the SMC (e.g. Perren, Piatti & Vázquez 2017). The SMC cluster population is also important to help understanding the interactions with the Large Magellanic Cloud (LMC) that seem to have caused some bursts of cluster formation (e.g. Piatti et al. 2011). The information on the early SMC evolution since the SMC–LMC interactions started to happen is not yet well constrained because there is a lack of SMC clusters older than ∼8 Gyr (Piatti 2011; Parisi et al. 2014). Therefore, it is of prime importance to derive accurate ages for candidates to be the oldest star clusters in the SMC.

Crowl et al. (2001) showed with *HST* data that the populous old clusters in the SMC span ages from 1 Gyr to the NGC 121 age (10.5–11.8 Gyr, Glatt et al. 2008), which is comparable to the ages of Galactic globular clusters. NGC 121 is the only known massive cluster older than 8 Gyr, but the SMC contains a much larger population of intermediate to low-mass clusters to be explored (e.g.

Gatto et al. 2021). Attempts to derive ages from ground-based data (e.g. Glatt, Grebel & Koch 2010) were hampered by the photometric limit hardly attaining the main-sequence turnoff (MSTO).

The VISCACHA (VIsible Soar photometry of star Clusters in tApii and Coxi HuguA; Maia et al. 2019, hereafter Paper I) survey is an ongoing project that employs the 4.1-m Southern Astrophysical Research (SOAR) telescope aided by adaptive optics that provides photometry deeper than the MSTO of old Magellanic Clouds clusters and resolved stars in the cluster cores. The VISCACHA data are designed to derive accurate ages and masses of the oldest intermediate to low-mass clusters of the SMC.

In this work, we analyse three old cluster candidates from Bica et al. (2020) catalogue. Clusters RZ 82 and RZ 158 (Rafelski & Zaritsky 2005) had integrated colours suggesting an intermediate or old age. Piatti (2011) estimated an age of 9.3 Gyr for HW 42 with Washington photometry at Blanco telescope. Perren et al. (2017) found that HW 42 might be as old as 5 Gyr with a total photometric mass of 200 $M_\odot$ with the same data. The VISCACHA data for these clusters were obtained to improve on these age, metallicity, and cluster mass estimates.

In Section 2, we present the observations and reductions, with the obtained *BVI* images. In Section 3, we discuss the statistical

Table 1. Log of observations for the three analysed clusters.

Cluster	RA (J2000) (h:m:s)	Dec. (J2000) (°:′:″)	Date	Instrument	Filters	Exp. time (s)	Seeing (arcsec)	FWHM (arcsec)	Airmass
RZ 82	00:53:09.6	−71:59:43	2018/12/12	SAMI	V, I	3x400, 3x600	0.80	0.81, 0.69	1.38
HW 42	01:01:06.3	−74:04:32	2018/10/06	SAMI	V, I	3x400, 3x600	0.85	0.90, 0.63	1.53
RZ 158	01:06:45.0	−74:49:58	2021/11/08	SAMI	V, I	3x400, 3x600	0.60	0.72, 0.63	1.45

Figure 1. Colour composite images of RZ 82 (left), HW 42 (middle), and RZ 158 (right) made from SAMI exposures. The images have 3 arcmin× 3 arcmin, corresponding to the SAMI FoV. North is up and East to the left.
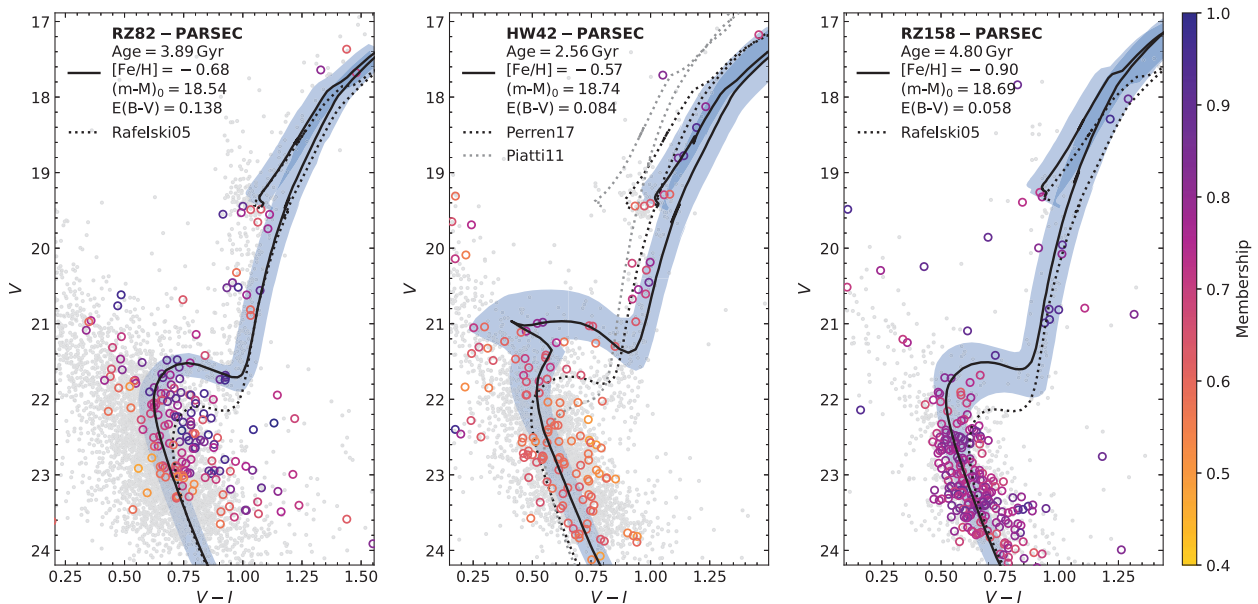
Figure 2. Decontaminated V versus $V - I$ CMDs with the isochrone fitting results for the three sample clusters. The best-fitting isochrone is shown as a solid line, whereas the surrounding blue region covers all the possible solutions within 1σ. The dashed isochrones give a comparison with previous literature results (see Table 2), assuming our derived distances and a suitable reddening when not available.

isochrone fitting. The clusters' masses are presented in Section 4. A discussion is given in Section 5 and the conclusions are drawn in Section 6.

2 OBSERVATIONS AND REDUCTIONS

The observations were carried out with the 4.1-m telescope SOAR, employing the SOAR Adaptive Module (Tokovinin et al. 2016) with ground-layer adaptive optics and the associated imager (SAMI).

We used standard reductions with bias subtraction and flat-field correction. GSC2.3 (Lasker et al. 2008) was used for the astrometric calibration while standard fields from Stetson (2000) were observed for photometric calibrations. More details are given in Paper I. Table 1 summarizes the observational information.

Fig. 1 shows the combined cluster images according to Table 1. Fig. 2 shows the respective CMDs, from where it becomes clear that the faintest stars reach around $V \sim 23.5$ mag for the three clusters, indicating an unprecedented photometry performance in terms of

Table 2. Isochrone fitting results derived with the SIRIUS code. The values correspond to the median and 1σ level of the posterior distribution. Literature results are presented for comparison: Rafelski & Zaritsky (2005, RZ05), Piatti (2011, P11), Perren et al. (2017, P17).

Cluster		Age (Gyr)	[Fe/H]	d (kpc)	A_V (mag)
RZ 82	(this work)	$3.9^{+0.8}_{-0.8}$	$-0.68^{+0.33}_{-0.33}$	$51.1^{+4.5}_{-4.5}$	$0.43^{+0.22}_{-0.22}$
	(RZ05)	$7.1^{+0.7}_{-2.5}$	-0.58	–	–
HW 42	(this work)	$2.6^{+0.3}_{-0.3}$	$-0.57^{+0.37}_{-0.37}$	$56.0^{+4.1}_{-4.1}$	$0.26^{+0.26}_{-0.26}$
	(P11)	$9.3^{+1.5}_{-1.5}$	$-1.40^{+0.25}_{-0.25}$	$60.3^{+2.8}_{-2.8}$	$0.09^{+0.03}_{-0.03}$
	(P17)	$5.0^{+5.0}_{-2.5}$	$-0.88^{+0.65}_{-0.65}$	$61.4^{+1.7}_{-1.7}$	$0.05^{+0.02}_{-0.02}$
RZ 158	(this work)	$4.8^{+1.6}_{-1.3}$	$-0.90^{+0.43}_{-0.39}$	$54.7^{+3.5}_{-3.5}$	$0.18^{+0.16}_{-0.12}$
	(RZ05)	$8.3^{+1.7}_{-0.4}$	-0.58	–	–

depth and spatial resolution, compared to literature data. Although faint, the clusters have relatively well-defined structures, with a core density that contrasts with the surroundings.

3 STATISTICAL ISOCHRONE FITTING

An important first step to carry out a reliable isochrone fitting is the assignment of a membership probability for the observed stars, removing the most likely to belong to the field population. Since the proper motion data from *Gaia* and other surveys are not deep enough for SMC clusters, we obtain the membership from a statistical analysis based on Maia, Corradi & Santos (2010), comparing the distance to the centre and local density of the stars in the CMD of the cluster sample (within the tidal radius) with a nearby field.

We employed the SIRIUS code (Souza et al. 2020) to the decontaminated V versus $V - I$ CMDs, comparing the observed distribution of stars to theoretical PARSEC isochrones (Bressan et al. 2012). A geometrical likelihood was applied for each star in a Markov Chain Monte Carlo sampling, using the membership probability and the number of stars around it on the CMD as a uniform prior. The magnitude of the red clump (RC) stars was also adopted as a Gaussian prior in $(m - M)_0$, in order to match the RC of the isochrone according to the metallicity. Age, metallicity, distance, and reddening are free parameters during the fitting process. The SIRIUS code was previously employed to VISCACHA (Dias et al. 2021, 2022, hereafter Paper III, Paper IV) and *HST* globular cluster data (e.g. Kerber et al. 2019; Oliveira et al. 2020; Souza et al. 2020, 2021), as well as to e.g. VVV, *Gaia,* and 2MASS data (Fernández-Trincado et al. 2021a, b). Table 2 contains the derived parameters and 1σ uncertainties obtained from the posterior distributions.

Fig. 2 presents the decontaminated V versus $V - I$ CMDs of RZ 82, HW 42, and RZ 158 with the best-fitting isochrones and 1σ region. Member stars are colour-coded with the membership probability and field stars are shown in grey (Maia et al. 2010). We also present an isochrone with the parameters from the literature (Rafelski & Zaritsky 2005; Piatti 2011; Perren et al. 2017), showing that VISCACHA data rule out the possibility of an old age. Fig. 3 presents the respective corner plots, with the posterior distributions of the free parameters in the diagonal panels and the correlations between them in the other panels.

The derived ages of 3.9, 2.6, and 4.8 Gyr for RZ 82, HW 42, and RZ 158 are considerably younger than the previous literature values, thus redefining a brighter turnoff with the present deep, decontaminated VISCACHA photometry. Nevertheless, the three clusters have a 'Gyr morphology', with some blue stragglers and

a red clump at $V \sim 19.4$ mag. The derived distances are suggestive of the location of the clusters relative to the SMC: 51.1 kpc for RZ 82, which is projected in the foreground of the SMC bulk population (62 kpc; De Grijs & Bono 2015), as illustrated by the crowded field in Fig. 1; ~55 kpc for HW 42 and RZ 158, which are located in the Southern Bridge. Concerning the metallicity, the only spectroscopic value available to date is for HW 42, for which De Bortoli et al. (2022) derived [Fe/H] $= -0.58 \pm 0.03$ from CaT analysis, in excellent agreement with the photometric metallicity found in the present work. RZ 158 shows a double peaked age-metallicity distribution in Fig. 3. Preliminary spectroscopic metallicity of [Fe/H] $= -1.06 \pm 0.10$ dex, Dias et al. (in preparation) supports the older peak around 5.5 Gyr, and not the peak around 4.0 Gyr, which is still consistent with the conclusions of the present work.

4 CLUSTER MASSES

We followed the procedures described in (Santos et al. 2020, hereafter Paper II) to derive total mass for the clusters. In summary, we determined their integrated apparent V magnitudes (V_{int}) by integrating the surface brightness profile from the centre out to the limiting radius, where the profile merges with the field stars surface brightness. We then converted V_{int} to the absolute one (M_V) by using the clusters' individual distance and extinction from isochrone fitting (Table 2). Finally, the mass and its uncertainty was calculated following the calibration with age and metallicity (fixed at $Z = 0.004$) of simple stellar population models given in Maia, Piatti & Santos (2014) and Paper II. Mass uncertainty comes from propagation of errors in the measured surface brightness (propagated to M_V error), age, extinction, and distance. The integrated properties are shown in Table 3.

5 DISCUSSION

The SMC clusters RZ 82, HW 42, and RZ 158 analysed in this work are three of the oldest from the Bica et al. (2020) catalogue, with ages of 7.1, 9.3, and 8.3 Gyr old, respectively, based on integrated light or shallower photometry. We have shown that these clusters are actually 3.9, 2.6, and 4.8 Gyr old, respectively, based on deeper and spatially resolved photometry. Some implications of the younger ages for these clusters are discussed below.

The present clusters are consistent with the overall SMC enrichment history (e.g. Paper III). Fig. 4 shows the age-metallicity relation of all SMC star clusters with available metallicities obtained with Ca II triplet technique, all in the same scale, combined with ages from the best CMD with isochrone fitting available, some of them using *HST* data (see compilation at Parisi et al. 2022). There is a large metallicity dispersion that is also seen in the multiple attempts of chemical evolution models to reproduce the SMC chemical evolution (e.g. De Bortoli et al. 2022). The three clusters analysed in this work were supposedly among the oldest according to previous works (see compilation at Bica et al. 2020). In particular, RZ 82 and RZ 158 had a combination of ages and metallicities that were off the bulk of SMC clusters and chemical enrichment models and the new ages and metallicities follow the trends now. HW 42 had two previous determinations of age and metallicities, both in apparent agreement with the SMC evolution, which made it difficult for spotting any issue. Our new age and metallicity for this cluster says that it was formed more recently when the SMC was more metal-rich. In fact, our results are supported

by the spectroscopic metallicity. In summary, the age-metallicity relation of the SMC is sensitive to the diverse source of parameters,
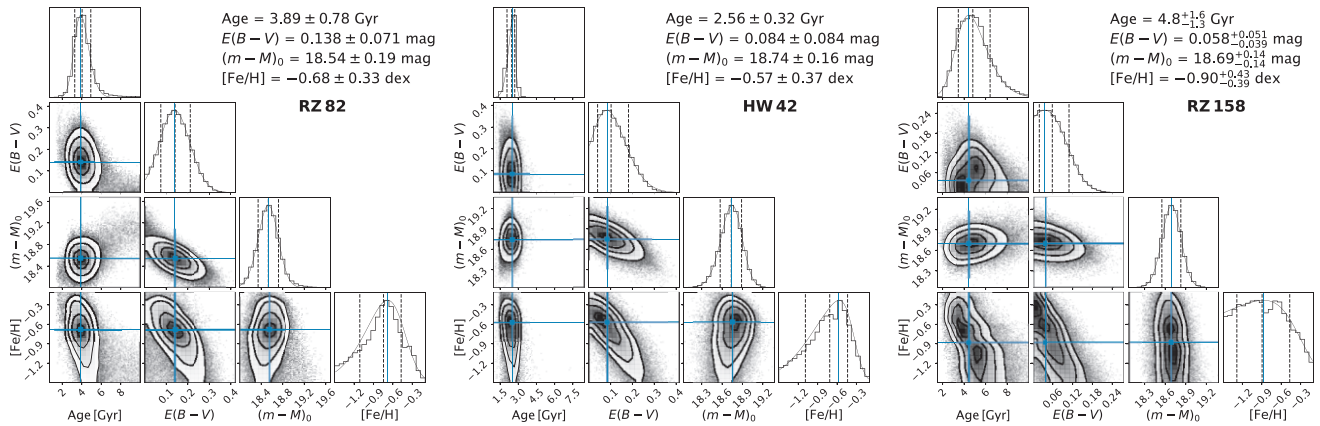
Figure 3. Corner plot of the resulting isochrone fits for the three sample clusters. The dashed lines in the histograms correspond to the median and the 16th and 84th percentiles as the 1σ levels. The contours in the 2D panels encompass the $[0.5\sigma, 1.0\sigma, 1.5\sigma, 2.0\sigma]$ levels. The posterior distributions in age shows that some walkers explore ages up to 10 Gyr, but the convergence is obtained in lower ages.

Table 3. Integrated magnitudes and masses of investigated clusters.

Cluster	V_{int}	M_V	$\log(M/M_\odot)$
RZ 82	13.57 ± 0.17	-5.39 ± 0.32	4.05 ± 0.17
HW 42	13.55 ± 0.09	-5.45 ± 0.32	3.97 ± 0.17
RZ 158	14.21 ± 0.22	-4.77 ± 0.30	3.88 ± 0.18
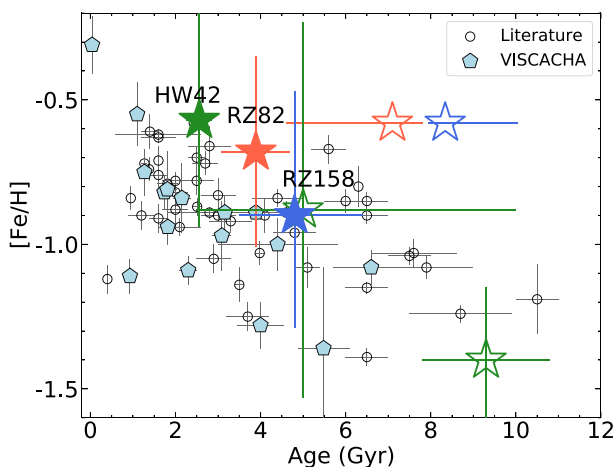
Figure 4. The age-metallicity relation of SMC star clusters. Black circles correspond to a literature compilation of homogeneous Ca II triplet spectroscopic metallicities by Da Costa & Hatzidimitriou (1998), Parisi et al. (2009), Parisi et al. (2015), Parisi et al. (2022), De Bortoli et al. (2022), and ages from Paper III, Paper IV; Mighell, Sarajedini & French (1998), Piatti et al. (2001), Piatti et al. (2005), Rafelski & Zaritsky (2005), Glatt et al. (2008), Livanou et al. (2013), Dias et al. (2014), Parisi et al. (2014), Li et al. (2016), Nayak et al. (2018), Lagioia et al. (2019), Narloch et al. (2021). Previous VISCACHA results from Paper I, Paper III, Paper IV are shown as blue pentagons. The filled stars are the clusters analysed in this work, whereas the empty stars are the same clusters but with the older ages and different metallicities from the literature (see the text for details).

and it will be best traced by homogeneous and accurate parameters as provided by the VISCACHA survey. Moreover, all the SMC clusters older than ~7 Gyr are more metal-poor than [Fe/H] ≲ −1.0.
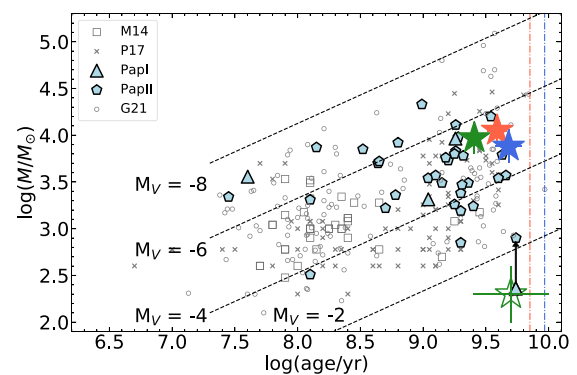

Figure 5. The age-mass relation of SMC star clusters. Literature data display the parameter space analysed by Maia et al. (2014, M14), Perren et al. (2017, P17), Paper I, Santos et al. (2020, Pap II), Gatto et al. (2021, G21). The iso-magnitude reference lines were adopted from M14 with metallicity [Fe/H] ∼ −0.7. The blue triangle in the bottom right is AM 3 with a lower limit mass from Pap I and integrated mass from Pap II indicated by the arrow. The three clusters analysed here are shown as filled stars as in Fig. 4. The empty star indicates the HW 42 parameters by P17. The vertical blue and red lines show the ages for RZ 82 and RZ 158. There is no previous published masses for these clusters.

The later evolution ($\tau \gtrsim 10^8$ yr) of star clusters involves the escape of stars by internal two body relaxation, commonly known as evaporation (see e.g. Fall, Chandar & Whitmore 2009). Low-mass stars are preferentially lost because the tendency that clusters have to reach energy equipartition combined with mass segregation, see e.g. Baumgardt & Makino (2003), Kruijssen & Lamers (2008). In this context, we have been searching for evolved star clusters that are missing low-mass stars, such as AM 3 already identified in Paper I.

It has been argued that the evaporation of star clusters does not depend on their total mass (Chandar, Fall & Whitmore 2010). Nevertheless, the only cluster from the VISCACHA sample showing signs of dissolution so far is a relatively old and low-mass cluster, AM 3 (Paper I), i.e. an outlier in the age-mass parameter space (see Fig. 5). HW 42 was previously analysed by Perren et al. (2017), with properties akin to AM 3 in Fig. 5, which would be very interesting. However, our determination of a younger age by a factor of two and almost two orders of magnitude heavier mass places the cluster within the parameter space of the bulk of star clusters, not being an

outlier anymore. RZ 82 and RZ 158 had age determinations placing them as outliers in Fig. 5 regardless their mass, however, our new determination of ages and masses for these two clusters are also consistent with the bulk of intermediate-age SMC clusters.

6 CONCLUSIONS

We studied CMDs of the faint SMC clusters RZ 82, HW 42, and RZ 158. The SOAR deep CMDs show well the turnoff regions, like in Paper I. The present ages of about 2–5 Gyr, are thus not as old as NGC 121 which remains as the only SMC cluster with genuine CMD counterpart of Galactic globular clusters. The present clusters show metallicities of [Fe/H] ~ -0.60 for RZ 82 and HW 42, and [Fe/H] $= -0.90$ for RZ 158. They fit well the cluster enrichment history of the SMC.

DATA AVAILABILITY

The data underlying this article are available in the NOIRLab Astro Data Archive (https://astroarchive.noirlab.edu/) or upon reasonable request to the authors.

REFERENCES

Baumgardt H., Makino J., 2003, MNRAS, 340, 227
Bica E., Westera P., Kerber L. D. O., Dias B., Maia F., Santos J. F. C., Jr, Barbuy B., Oliveira R. A. P., 2020, AJ, 159, 82
Bressan A., Marigo P., Girardi L., Salasnich B., Dal Cero C., Rubele S., Nanni A., 2012, MNRAS, 427, 127
Chandar R., Fall S. M., Whitmore B. C., 2010, ApJ, 711, 1263
Crowl H. H., Sarajedini A., Piatti A. E., Geisler D., Bica E., Clariá J. J., Santos J. F. C., Jr, 2001, AJ, 122, 220
Da Costa G. S., Hatzidimitriou D., 1998, AJ, 115, 1934
De Bortoli B. J., Parisi M. C., Bassino L. P., Geisler D., Dias B., Gimeno G., Angelo M. S., Mauro F., 2022, A&A, 664, 11
De Grijs R., Bono G., 2015, AJ, 149, 179
Dias B., Kerber L. O., Barbuy B., Santiago B., Ortolani S., Balbinot E., 2014, A&A, 561, A106
Dias B. et al., 2021, A&A, 647, L9 (Paper III)
Dias B. et al., 2022, MNRAS, 512, 4334 (Paper IV)
Fall S. M., Chandar R., Whitmore B. C., 2009, ApJ, 704, 453
Fernández-Trincado J. G. et al., 2021a, A&A, 647, A64
Fernández-Trincado J. G. et al., 2021b, ApJ, 908, L42
Gatto M. et al., 2021, MNRAS, 507, 3312
Glatt K. et al., 2008, AJ, 135, 1106
Glatt K., Grebel E. K., Koch A., 2010, A&A, 517, A50
Kerber L. O. et al., 2019, MNRAS, 484, 5530
Kruijssen J. M. D., Lamers H. J. G. L. M., 2008, A&A, 490, 151
Lagioia E. P., Milone A. P., Marino A. F., Dotter A., 2019, ApJ, 871, 140
Lasker B. M. et al., 2008, AJ, 136, 735
Li C., de Grijs R., Deng L., Geller A. M., Xin Y., Hu Y., Faucher-Giguère C.-A., 2016, Nature, 529, 502
Livanou E., Dapergolas A., Kontizas M., Nordström B., Kontizas E., Andersen J., Dirsch B., Karampelas A., 2013, A&A, 554, A16
Maia F. F. S., Corradi W. J. B., Santos J. F. C., Jr, 2010, MNRAS, 407, 1875
Maia F. F. S., Piatti A. E., Santos J. F. C., 2014, MNRAS, 437, 2005
Maia F. F. S. et al., 2019, MNRAS, 484, 5702 (Paper I)
Mighell K. J., Sarajedini A., French R. S., 1998, AJ, 116, 2395
Narloch W. et al., 2021, A&A, 647, A135
Nayak P. K., Subramaniam A., Choudhury S., Sagar R., 2018, A&A, 616, A187
Oliveira R. A. P. et al., 2020, ApJ, 891, 37
Parisi M. C., Grocholski A. J., Geisler D., Sarajedini A., Clariá J. J., 2009, AJ, 138, 517
Parisi M. C. et al., 2014, AJ, 147, 71
Parisi M. C., Geisler D., Clariá J. J., Villanova S., Marcionni N., Sarajedini A., Grocholski A. J., 2015, AJ, 149, 154
Parisi M. C., Gramajo L. V., Geisler D., Dias B., Clariá J. J., Da Costa G., Grebel E. K., 2022, A&A, 662, 16
Perren G. I., Piatti A. E., Vázquez R. A., 2017, A&A, 602, A89
Piatti A. E., 2011, MNRAS, 416, L89
Piatti A. E., Santos J. F. C., Clariá J. J., Bica E., Sarajedini A., Geisler D., 2001, MNRAS, 325, 792
Piatti A. E., Santos J. F. C., Jr, Clariá J. J., Bica E., Ahumada A. V., Parisi M. C., 2005, A&A, 440, 111
Piatti A. E., Clariá J. J., Bica E., Geisler D., Ahumada A. V., Girardi L., 2011, MNRAS, 417, 1559
Rafelski M., Zaritsky D., 2005, AJ, 129, 2701
Santos João F. C. J. et al., 2020, MNRAS, 498, 205 (Paper II)
Souza S. O., Kerber L. O., Barbuy B., Pérez-Villegas A., Oliveira R. A. P., Nardiello D., 2020, ApJ, 890, 38
Souza S. O. et al., 2021, A&A, 656, A78
Stetson P. B., 2000, PASP, 112, 925
Tokovinin A., Cantarutti R., Tighe R., Schurter P., Martinez M., Thomas S., van der Bliek N., 2016, PASP, 128, 125003

This paper has been typeset from a TEX/LATEX file prepared by the author.